OPTIMAL ZERO FORCING PRECODER AND DECODER DESIGN FOR MULTI-USER MIMO FBMC UNDER STRONG CHANNEL SELECTIVITY

*François Rottenberg†, Xavier Mestre††, Jérôme Louveaux†

†ICTEAM, Université Catholique de Louvain
Place du Levant, 2, B-1348 Louvain-la-Neuve, Belgium
††Centre Tecnològic de Telecomunicacions de Catalunya
Av. Carl Friedrich Gauss, 7, 08860 Castelldefels, Spain

ABSTRACT

This paper investigates the optimal design of precoders or decoders under a channel inversion criterion for multi-user (MU) MIMO filterbank multicarrier (FBMC) modulations. The base station (BS) is assumed to use a single tap precoding/decoding matrix at each subcarrier in the downlink/uplink, resulting in a low complexity of implementation. The expression of the asymptotic mean squared error (MSE) for this precoding/decoding design in the case of strong channel selectivity is recalled and simplified. Optimizing the MSE under a channel inversion constraint, the expression of the optimal precoding/decoding matrix is found. It is shown that as long as the number of BS antennas is larger than the number of users, the optimized precoder and decoder can compensate for the channel frequency selectivity and even restore the system orthogonality for a large enough number of BS antennas.

Index Terms— FBMC, MU MIMO, precoder, decoder, strong channel selectivity.

1. INTRODUCTION

Offset-QAM based Filter Bank Multi-Carrier (FBMC-OQAM) has been shown to be an interesting alternative to Cyclic Prefix-based Orthogonal Frequency Division multiplexing (CP-OFDM) for the physical layer of new communications systems. At the cost of increased complexity and reconstruction delay, FBMC-OQAM uses filters with a much better time and frequency localization than CP-OFDM [1]. This in turn translates into higher spectral efficiency and relaxed synchronization constraints [2].

However, the combination of FBMC-OQAM with MIMO technologies is not as straightforward as in CP-OFDM, especially in the case of high channel frequency selectivity. Indeed, the channel selectivity destroys the system orthogonality and creates distortion in the received waveform [3, 4]. Many works in the literature have investigated this problem [4–7]. Most of the approaches are based on the design of multi-tap fractionally spaced equalizers. For instance, in [8] the authors designed multi-tap decoding matrices following a frequency sampling design. On the other hand, [9] proposes a multi-tap filtering solution at both transmit and receive sides. The work originally devised for the SISO case in [3] and later extended for the MIMO case in [10] proposes instead a parallel multi-stage processing architecture at both sides of the communication link. One should however note that multi-tap filtering and multi-stage processing increase the complexity of the system.

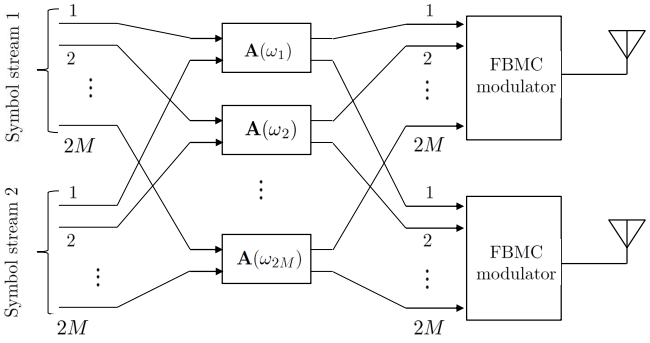

Fig. 1. Single tap per-subcarrier precoding at the base station in downlink.

In this paper, we propose a very low complexity approach based on simple one tap per-subcarrier precoding and decoding matrices. We show that even with a such simple structure, one can exploit the degrees of freedom offered by the extra BS antennas to restore the system orthogonality.

We consider a MU MIMO system with one base station (BS) equipped with N antennas and N_U users, each one equipped with a single antenna and not able to cooperate with each other[1]. The number of streams is N_U with $N \geqslant N_U$. The channel frequency response matrix $\boldsymbol{H}(\omega)$ is assumed to be perfectly known by the BS. For the sake of clarity, $\boldsymbol{H}(\omega)$ is denoted $\boldsymbol{H}_{\mathrm{DL}}(\omega) \in \mathbb{C}^{N_U \times N}$ when referred to the specific downlink (DL) scenario and $\boldsymbol{H}_{\mathrm{UL}}(\omega) \in \mathbb{C}^{N \times N_U}$ resp. in the uplink (UL) case.

Multicarrier modulations divide the transmission band into multiple narrow bands. If the number of subcarriers is large with respect to the channel delay spread, a common assumption is to assume that the channel is approximately frequency flat inside each sub-band such that precoding and decoding operations can be performed at the subcarrier level. In DL, the BS applies a single tap per-subcarrier precoding matrix $\boldsymbol{A}(\omega_k) \in \mathbb{C}^{N \times N_U}$ with $\omega_k = \frac{2\pi(k-1)}{2M}$ to pre-equalize the channel, as depicted in Fig. 1. In UL, the BS applies a single tap per-subcarrier decoding matrix $\boldsymbol{B}(\omega_k) \in \mathbb{C}^{N_U \times N}$ to equalize the channel, as depicted in Fig. 2. Since users cannot collaborate, the precoding operations in UL and the decoding operations

*The research reported herein was partly funded by Fonds pour la Formation à la Recherche dans l'Industrie et dans l'Agriculture (F.R.I.A.) and by the Catalan and Spanish governments under grants 2014SGR1567 and TEC2014-59255-C3-1.

[1]Note that one could straightforwardly apply the results of this paper to a point-to-point (PTP) communication link.

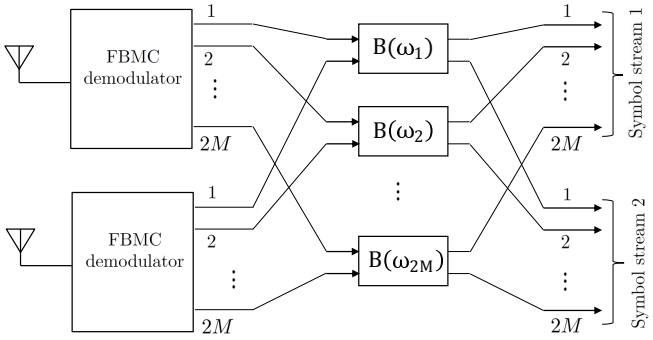

Fig. 2. Single tap per-subcarrier decoding at the base station in uplink.

in DL are assumed to be a real normalization scalar multiplication, as will be further detailed below.

The designs of Fig. 1 and Fig. 2 usually rely on channel frequency flatness at the subcarrier level. When the variation of the channel becomes non-negligible, this assumption becomes very inaccurate and distortion will appear. Nevertheless, in contrast to most of the typical approaches dealing with high frequency channel selectivity, we propose to keep the low complexity implementation of Fig. 1 and Fig. 2 based on a simple one tap per-subcarrier precoding or decoding matrix. However, we do not make the assumption that the channel is frequency flat at the subcarrier level and we characterize (and simplify) the expression of the mean squared error (MSE) based on the distortion approximation derived in [10]. Minimizing the MSE formula, the optimal ZF precoding and decoding matrices are found, taking into account the channel frequency selectivity. These optimized precoders and decoders can use the extra antennas of the BS, *i.e.* when $N > N_U$, to compensate for the distortion and even restore the system orthogonality.

2. MSE FORMULATION FOR FBMC-OQAM UNDER CHANNEL FREQUENCY SELECTIVITY

We consider a FBMC-OQAM system with $2M$ subcarriers. The prototype filter $p[n]$ is assumed even symmetric and identical at transmitter and receiver sides. It has length $2M\kappa$, where κ is the overlapping factor. The pulse is assumed to result from the discretization of a smooth analog waveform $p(t)$, so that $p'[n]$ denotes the discretization of the derivative of $p(t)$. Furthemore, the pulse $p[n]$ is assumed to be constructed so as to meet the perfect reconstruction (PR) constraints [11], *i.e.* perfect orthogonality after demodulation under frequency flat channel conditions[2].

To be able to give an analytical expression of the MSE at the analysis filterbank output, $\boldsymbol{H}(\omega)$, $\boldsymbol{A}(\omega)$ and $\boldsymbol{B}(\omega)$ are assumed to be smooth functions of ω. The actual precoding and decoding matrices implemented in Fig. 1 and Fig. 2 at the k-th subcarrier result from the evaluation of the functions $\boldsymbol{A}(\omega)$ and $\boldsymbol{B}(\omega)$ at frequency $\omega_k = \frac{2\pi(k-1)}{2M}$. Furthermore, a ZF criterion over the global transmission chain is assumed, meaning that $\boldsymbol{B}(\omega)\boldsymbol{H}(\omega)\boldsymbol{A}(\omega) = \boldsymbol{I}_{N_U}$ where $\boldsymbol{I}_{N_U}$ is the $N_U \times N_U$ identity matrix. The complex transmitted symbols are bounded i.i.d. random variables with zero mean and unit variance.

[2]In practice, even if the filter is of the nearly perfect reconstruction type, the presented distortion formula remains a good approximation, as will be shown in the simulations.

Under the previous assumptions and for a large number of subcarriers, an expression of the asymptotic distortion was given in [10] for the case of different pulses at transmitter and receiver sides. In the more specific case considered here, the total MSE at subcarrier k can be written as follows

$$\begin{aligned}\mathrm{MSE}(k) = &\frac{2\eta_{1010}^{(+,-)}}{(2M)^2}\mathrm{tr}\left[\left(\boldsymbol{BHA}'\right)\left(\boldsymbol{BHA}'\right)^H\right]\\ &+\frac{2\eta_{0101}^{(-,+)}}{(2M)^2}\mathrm{tr}\left[\left(\boldsymbol{B}'\boldsymbol{HA}\right)\left(\boldsymbol{B}'\boldsymbol{HA}\right)^H\right]\\ &-\frac{4\eta_{1001}^{(-,+)}}{(2M)^2}\mathrm{tr}\left[\Re\left(\boldsymbol{BHA}'\right)\Re^T\left(\boldsymbol{B}'\boldsymbol{HA}\right)\right]\\ &-\frac{4\eta_{1001}^{(+,-)}}{(2M)^2}\mathrm{tr}\left[\Im\left(\boldsymbol{BHA}'\right)\Im^T\left(\boldsymbol{B}'\boldsymbol{HA}\right)\right]\\ &+N_0\mathrm{tr}\left[\boldsymbol{BB}^H\right]+O\left((2M)^{-2}\right) \qquad (1)\end{aligned}$$

where N_0 is the noise variance. For the sake of clarity, from now on, we drop the subcarrier frequency index, *i.e.* $\boldsymbol{B}$, $\boldsymbol{H}$, $\boldsymbol{A}$ and $\boldsymbol{B}'$, $\boldsymbol{H}'$, $\boldsymbol{A}'$ refer, respectively, to the frequency response and the corresponding derivative of the decoder, channel and precoder matrices, evaluated at subcarrier frequency $\omega_k = \frac{2\pi(k-1)}{2M}$. The different coefficients $\eta_{----}^{(\pm,\mp)}$ appearing in (1) are pulse-related quantities defined in the appendix. In a practical system, the number of subcarriers is large enough such that (1) is a very good approximation of the distortion, as will be shown in the simulations.

A first contribution of this paper is the following proposition that greatly simplifies the previous expression.

Proposition 2.1 *Using asymptotic equivalence of the η's when $2M \to +\infty$, the above* MSE *expression can be simplified to*

$$\begin{aligned}\mathrm{MSE}(k) = &\alpha tr\left[\left(\boldsymbol{BH}'\boldsymbol{A}\right)\left(\boldsymbol{BH}'\boldsymbol{A}\right)^H\right]\\ &-(2\alpha+2\beta)tr\left[\Im(\boldsymbol{BHA}')\Im(\boldsymbol{B}'\boldsymbol{HA})^T\right]\\ &+N_0 tr\left[\boldsymbol{BB}^H\right]+O\left(2M^{-2}\right) \qquad (2)\end{aligned}$$

where $\alpha = \frac{2|\eta_{1010}^{(+,-)}|}{(2M)^2}$ and $\beta = \frac{2|\eta_{1001}^{(+,-)}|}{(2M)^2}$.

Proof: In order to prove this proposition, it is sufficient to show that $\eta_{1010}^{(+,-)} = \eta_{0101}^{(-,+)}$ and that $\eta_{1001}^{(-,+)} \to \eta_{1010}^{(+,-)}$ as $2M \to +\infty$. The fact that $\eta_{1010}^{(+,-)} = \eta_{0101}^{(-,+)}$ is proven in Corollary 1 of [3]. As for the second identity, one can prove it by using the fact that the prototype pulses are discretized versions of the corresponding differentiable waveforms. Details are omitted due to space constraints.

3. OPTIMAL LINEAR DECODER AND PRECODER

We now optimize the above MSE formulation to find the expression of the optimal single tap per-subcarrier precoding and decoding matrices for frequency selective channel. While optimizing the decoder in UL (resp. precoder in DL), the precoder (resp. decoder) at the other end is assumed to be a real positive scalar $\xi(\omega)$. This assumption makes sense since the users cannot collaborate. The value $\xi(\omega)$ is fixed to ensure the following per-subcarrier transmit power constraint together with the considered channel inverting constraint, namely

$$\begin{aligned}\mathrm{tr}(\boldsymbol{AA}^H) &= P_T\\ \boldsymbol{BHA} &= \boldsymbol{I}_{N_U}. \qquad (3)\end{aligned}$$

3.1. Optimal linear decoder (Multiple Access Channel, uplink)

In the UL case, $\boldsymbol{H}_{\mathrm{UL}}, \boldsymbol{H}'_{\mathrm{UL}} \in \mathbb{C}^{N \times N_U}$ correspond to the tall channel frequency response and its derivative evaluated at the subcarrier of interest. From the power normalization and channel inversion constraints, the general solution of the problem (3) can be written in the following form

$$\begin{aligned} \boldsymbol{A}_{\mathrm{UL}} &= \xi_{\mathrm{UL}} \boldsymbol{I}_{N_U} \\ \boldsymbol{B}_{\mathrm{UL}} &= \frac{1}{\xi_{\mathrm{UL}}} \boldsymbol{H}^{\dagger} + \frac{1}{\xi_{\mathrm{UL}}} \tilde{\boldsymbol{B}} \boldsymbol{P}^{\dagger} \end{aligned} \tag{4}$$

where $\boldsymbol{H}^{\dagger} = (\boldsymbol{H}_{\mathrm{UL}}^H \boldsymbol{H}_{\mathrm{UL}})^{-1} \boldsymbol{H}_{\mathrm{UL}}^H$, $\xi_{\mathrm{UL}} = \sqrt{P_T / N_U}$, $\boldsymbol{P}^{\dagger} = \boldsymbol{I}_N - \boldsymbol{H}_{\mathrm{UL}} \boldsymbol{H}^{\dagger}$, and where $\tilde{\boldsymbol{B}}$ is an $N_U \times N$ matrix to be optimized. This shows that the optimal decoder can be written as the left pseudo inverse of the channel plus a matrix lying on the left null space of $\boldsymbol{H}_{\mathrm{UL}}$. In the trivial case $N = N_U$, the decoder is the inverse of the channel since there are no extra degrees of freedom.

One can check that the second term of the distortion in (2) is null due to the fact that $\Im(\boldsymbol{B}_{\mathrm{UL}} \boldsymbol{H}_{\mathrm{UL}} \boldsymbol{A}'_{\mathrm{UL}}) = \Im(\xi'_{\mathrm{UL}} / \xi_{\mathrm{UL}} \boldsymbol{I}_{N_U}) = \boldsymbol{0}$ with ξ_{UL} purely real and frequency independent. Therefore, the optimization problem can be turned into the minimization of a quadratic expression in $\tilde{\boldsymbol{B}}$

$$\begin{aligned} \min_{\tilde{\boldsymbol{B}}} \quad & \alpha \mathrm{tr}\left[\left(\boldsymbol{H}^{\dagger} \boldsymbol{H}'_{\mathrm{UL}} + \tilde{\boldsymbol{B}} \boldsymbol{P}^{\dagger} \boldsymbol{H}'_{\mathrm{UL}} \right) \left(\boldsymbol{H}^{\dagger} \boldsymbol{H}'_{\mathrm{UL}} + \tilde{\boldsymbol{B}} \boldsymbol{P}^{\dagger} \boldsymbol{H}'_{\mathrm{UL}} \right)^H \right] \\ & + \frac{N_0 N_U}{P_T} \mathrm{tr}\left[\left(\boldsymbol{H}_{\mathrm{UL}}^H \boldsymbol{H}_{\mathrm{UL}} \right)^{-1} + \tilde{\boldsymbol{B}} \boldsymbol{P}^{\dagger} \tilde{\boldsymbol{B}}^H \right]. \end{aligned} \tag{5}$$

Setting the derivative of this expression with respect to $\tilde{\boldsymbol{B}}^*$ to $\boldsymbol{0}$, we find that the optimum solution is such that

$$\tilde{\boldsymbol{B}} = -\boldsymbol{H}^{\dagger} \boldsymbol{H}'_{\mathrm{UL}} \left(\boldsymbol{H}'^H_{\mathrm{UL}} \boldsymbol{P}^{\dagger} \boldsymbol{H}'_{\mathrm{UL}} + \frac{N_0 N_U}{P_T \alpha} \boldsymbol{I}_{N_U} \right)^{-1} \boldsymbol{H}'^H_{\mathrm{UL}} \tag{6}$$

where we used the matrix inversion lemma.

3.2. Optimal linear precoder (Broadcast Channel, downlink)

In the DL case, $\boldsymbol{H}_{\mathrm{DL}}, \boldsymbol{H}'_{\mathrm{DL}} \in \mathbb{C}^{N_U \times N}$ refer to the fat channel frequency response and its derivative evaluated at the subcarrier of interest. From the constraints in (3), the general solution can be written as

$$\begin{aligned} \boldsymbol{A}_{\mathrm{DL}} &= \frac{1}{\xi_{\mathrm{DL}}} \boldsymbol{H}^{+} + \frac{1}{\xi_{\mathrm{DL}}} \boldsymbol{P}^{+} \tilde{\boldsymbol{A}} \\ \boldsymbol{B}_{\mathrm{DL}} &= \xi_{\mathrm{DL}} \boldsymbol{I}_{N_U} \end{aligned} \tag{7}$$

where $\boldsymbol{H}^{+} = \boldsymbol{H}_{\mathrm{DL}}^H (\boldsymbol{H}_{\mathrm{DL}} \boldsymbol{H}_{\mathrm{DL}}^H)^{-1}$, $\boldsymbol{P}^{+} = \boldsymbol{I}_N - \boldsymbol{H}^{+} \boldsymbol{H}_{\mathrm{DL}}$ and $\xi_{\mathrm{DL}} = \sqrt{\mathrm{tr}\left((\boldsymbol{H}_{\mathrm{DL}} \boldsymbol{H}_{\mathrm{DL}}^H)^{-1} + \tilde{\boldsymbol{A}}^H \boldsymbol{P}^{+} \tilde{\boldsymbol{A}} \right) / P_T}$. As in the above derivation, the second term of the distortion in (2) also disappears due to $\Im(\boldsymbol{B}'_{\mathrm{DL}} \boldsymbol{H}_{\mathrm{DL}} \boldsymbol{A}_{\mathrm{DL}}) = \Im(\xi'_{\mathrm{DL}} / \xi_{\mathrm{DL}} \boldsymbol{I}_{N_U}) = \boldsymbol{0}$ with ξ_{DL} purely real. The optimization problem simplifies to

$$\begin{aligned} \min_{\tilde{\boldsymbol{A}}} & \alpha \mathrm{tr}\left[\left(\boldsymbol{H}'_{\mathrm{DL}} \boldsymbol{H}^{+} + \boldsymbol{H}'_{\mathrm{DL}} \boldsymbol{P}^{+} \tilde{\boldsymbol{A}} \right)^H \left(\boldsymbol{H}'_{\mathrm{DL}} \boldsymbol{H}^{+} + \boldsymbol{H}'_{\mathrm{DL}} \boldsymbol{P}^{+} \tilde{\boldsymbol{A}} \right) \right] \\ & + \frac{N_0 N_U}{P_T} \mathrm{tr}\left[(\boldsymbol{H}_{\mathrm{DL}} \boldsymbol{H}_{\mathrm{DL}}^H)^{-1} + \tilde{\boldsymbol{A}}^H \boldsymbol{P}^{+} \tilde{\boldsymbol{A}} \right] \end{aligned} \tag{8}$$

the solution of which is, after applying matrix inversion lemma,

$$\tilde{\boldsymbol{A}} = -\boldsymbol{H}'^H_{\mathrm{DL}} \left(\boldsymbol{H}'_{\mathrm{DL}} \boldsymbol{P}^{+} \boldsymbol{H}'^H_{\mathrm{DL}} + \frac{N_0 N_U}{P_T \alpha} \boldsymbol{I}_{N_U} \right)^{-1} \boldsymbol{H}'_{\mathrm{DL}} \boldsymbol{H}^{+}. \tag{9}$$

One can check that the asymptotic MSE in (2) evaluated for the optimal precoder and decoder will be exactly the same if the channels are the Hermitian of one another, *i.e.* $\boldsymbol{H}_{\mathrm{UL}} = \boldsymbol{H}_{\mathrm{DL}}^H$.

3.3. Asymptotic analysis at low and high SNR

We concentrate here on the behavior of the optimum linear decoder in the uplink (MAC) channel. Similar conclusions also hold for the optimum precoder in the downlink (BC) channel. We assume that the number of users N_U and the transmit power P_T remain constant while we let N_0 go to 0 or $+\infty$ (high and low SNR respectively). At low SNR, the expression in (6) tends to 0 and the optimal decoder converges to

$$\lim_{N_0 \to \infty} \boldsymbol{B}_{\mathrm{UL}} = \frac{1}{\xi_{\mathrm{UL}}} \boldsymbol{H}^{\dagger}. \tag{10}$$

As could be expected, when the noise power is large, the distortion caused by channel selectivity is comparatively negligible. The best thing to do is to use the classical pseudo-inverse of the channel to combine the signals of each antenna.

At high SNR, the optimal decoder converges to a limit that depends on the rank of $\boldsymbol{P}^{\dagger}$. One can rewrite $\boldsymbol{P}^{\dagger}$ as a function of the SVD decomposition of $\boldsymbol{H}_{\mathrm{UL}}$

$$\boldsymbol{H}_{\mathrm{UL}} = \begin{bmatrix} \boldsymbol{U}_1 & \boldsymbol{U}_2 \end{bmatrix} \begin{bmatrix} \boldsymbol{\Sigma}_{N_U \times N_U} & \boldsymbol{0}^H_{N - N_U \times N_U} \end{bmatrix}^H \boldsymbol{V}^H. \tag{11}$$

We then find $\boldsymbol{P}^{\dagger} = \boldsymbol{U}_2 \boldsymbol{U}_2^H$ where $\boldsymbol{U}_2$ is the $N \times N - N_U$ matrix composed of the $N - N_U$ left singular vectors of $\boldsymbol{H}_{\mathrm{UL}}$ associated to its zeros singular values. It is then straightforward to see that the rank of $\boldsymbol{P}^{\dagger}$ is the dimension of the left null space of $\boldsymbol{H}_{\mathrm{UL}}$, *i.e.* $N - N_U$. Assuming that $\boldsymbol{H}'_{\mathrm{UL}}$ is full rank, two cases must be considered. First, if $N \geqslant 2N_U$, the limit becomes

$$\lim_{N_0 \to 0} \tilde{\boldsymbol{B}} = -\boldsymbol{H}^{\dagger} \boldsymbol{H}'_{\mathrm{UL}} \left(\boldsymbol{H}'^H_{\mathrm{UL}} \boldsymbol{P}^{\dagger} \boldsymbol{H}'_{\mathrm{UL}} \right)^{-1} \boldsymbol{H}'^H_{\mathrm{UL}}. \tag{12}$$

Replacing this expression of $\tilde{\boldsymbol{B}}$ into (5), it can be seen that the limit of the asymptotic MSE at high SNR will tend to zero. This means that for twice as many antennas as the number of served users, we can completely remove the first order approximation of the distortion caused by channel frequency selectivity.

As for the case $N < 2N_U$, using the fact that $\boldsymbol{P}^{\dagger} = \boldsymbol{U}_2 \boldsymbol{U}_2^H$, one can reapply the matrix inversion lemma on $\tilde{\boldsymbol{B}} \boldsymbol{P}^{\dagger}$ in order to show that the limit becomes

$$\lim_{N_0 \to 0} \tilde{\boldsymbol{B}} \boldsymbol{P}^{\dagger} = -\boldsymbol{H}^{\dagger} \boldsymbol{H}'_{\mathrm{UL}} \boldsymbol{H}'^H_{\mathrm{UL}} \boldsymbol{U}_2 \left(\boldsymbol{U}_2^H \boldsymbol{H}'_{\mathrm{UL}} \boldsymbol{H}'^H_{\mathrm{UL}} \boldsymbol{U}_2 \right)^{-1} \boldsymbol{U}_2^H. \tag{13}$$

In this case, the noise term of the MSE will tend to zero but the first order approximation of the distortion will only partially be compensated.

We can conclude that the optimal ZF decoder and precoder can be written in a compact expression as the pseudo inverse of the channel plus a matrix lying on the null space of the channel. This design can compensate for the degradation due to channel frequency selectivity and even completely remove the first order approximation of the distortion for twice as many BS antennas as the number of served users.

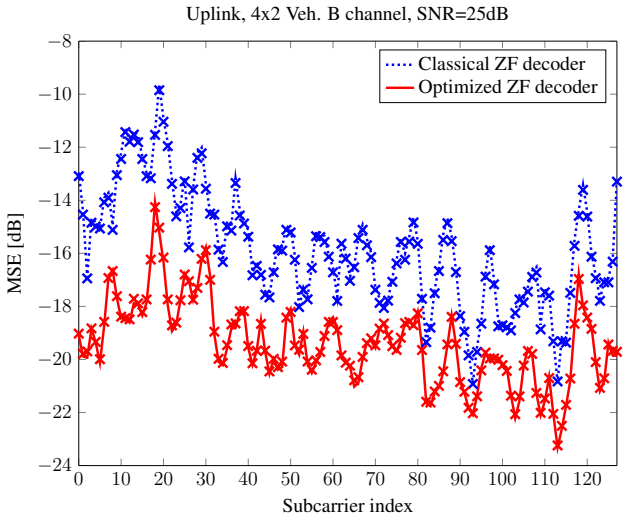

Fig. 3. The optimal ZF decoder clearly outperforms the classical ZF decoder. The asymptotic approximation of the MSE, represented in solid line, matches perfectly the simulated MSE, represented in crosses.

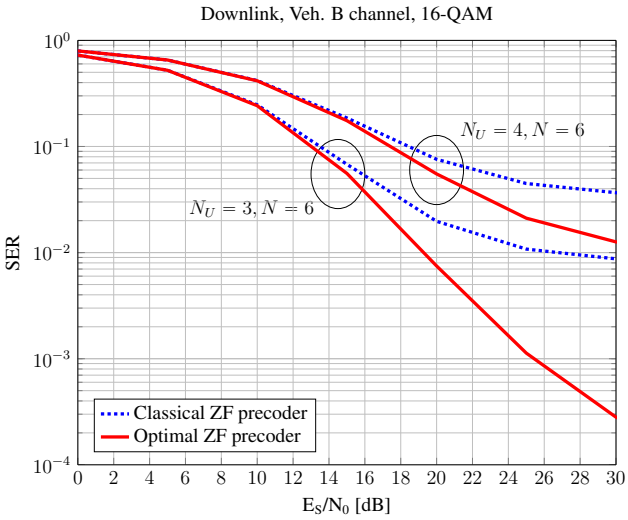

Fig. 4. SER comparison of the classical and optimal ZF precoders for a highly frequency selective channel.

4. SIMULATION RESULTS

The following simulations compare the performance of the optimized ZF precoders and decoders with respect to classical ZF precoders and decoders, strongly relying on the hypothesis of channel frequency flatness at the subcarrier level, *i.e.* the pseudo inverse of the channel. We consider a FBMC-OQAM system with $2M = 128$ subcarriers and subcarrier spacing $\Delta f = 15$kHz. The channels are randomly drawn from the ITU Vehicular B channel model, *i.e.* a highly frequency selective channel. Due to space constraints, no simulations are shown for a low frequency selective channel such as the ITU Vehicular A model. In this case, the performance of the classical and optimized structures would be similar given the small distortion induced by the channel. The Phydyas prototype pulse with overlapping factor $\kappa = 4$ is used in the simulations [12]. This pulse does not fully satisfy the PR constraints but is of the nearly-perfect-reconstruction (NPR) type. Given that it almost fulfills PR constraints, the derived MSE expression (2) remains a very good approximation of the distortion, as will be shown in the following.

Fig. 3 shows the MSE of the classical ZF decoder and the optimal ZF decoder. The BS is assumed to have $N = 4$ antennas serving $N_U = 2$ users and the SNR of the system is 25dB. One can first check that the simulated MSE (in cross markers) perfectly matches the theoretical approximation (in solid line) of (2). Furthermore, in the high SNR regime considered here, the classical ZF decoder is limited by the distortion induced by the channel frequency selectivity. On the other hand, the optimal ZF decoder uses the two extra antennas to cancel the distortion, providing a clear performance gain.

In Fig. 4, the symbol error rate (SER) for the classical and optimal FBMC precoders are plotted for different MU MIMO configurations. The SER saturates very quickly with a classical ZF precoder due to the very high channel frequency selectivity. On the other hand, using the optimal ZF precoder, the SER saturates at higher SNR in the $N_U = 4, N = 6$ case. In the case $N_U = 3, N = 6$, the SER does not even saturate in the considered SNR range since the BS has twice as many antennas and can completely remove the first order approximation of the distortion. This is in accordance with the asymptotic study at high SNR conducted in Section 3.3.

5. CONCLUSION

This work investigated the optimal design of ZF precoders and decoders for FBMC modulations in a MU MIMO context. The proposed method has a low complexity of implementation and can deal with high channel selectivity provided that the number of BS antennas is larger than the number of users. To obtain the optimal precoders and decoders, the expression of the asymptotic MSE was recalled and simplified. From the asymptotic study performed at high SNR, it appears that the first order approximation of the distortion can be completely removed if the number of BS antennas is twice as large as the number of users.

6. APPENDIX

We define here the pulse-related quantities $\eta^{(\pm,\mp)}_{----}$ appearing in the output MSE expressions in (1) and (2). For two general pulses $p[n]$ and $q[n]$, let $\boldsymbol{P}$ and $\boldsymbol{Q}$ denote the $2M \times \kappa$ matrices built by rearranging the original samples of $p[n]$ and $q[n]$ in columns. Next, consider the two $2M \times (2\kappa - 1)$ matrices $\mathcal{R}(p,q)$ and $\mathcal{S}(p,q)$ defined as

$$\begin{aligned}\mathcal{R}(p,q) &= \boldsymbol{P} \circledast \boldsymbol{J}_{2M}\boldsymbol{Q} \\ \mathcal{S}(p,q) &= (\boldsymbol{J}_2 \otimes \boldsymbol{I}_M)\boldsymbol{P} \circledast \boldsymbol{J}_{2M}\boldsymbol{Q}\end{aligned} \tag{14}$$

where $\circledast$ denotes the row-wise convolution between matrices, $\boldsymbol{J}_{2M}$ is the $2M \times 2M$ anti-identity matrix and where $\otimes$ denotes the Kronecker product. Given a prototype pulse $p[n]$, we define

$$\begin{aligned}\eta^{(+,-)}_{mnqr} = \frac{1}{2M}\mathrm{tr}\Big[&\mathcal{R}(p^{(m)},p^{(n)})\mathcal{R}^T(p^{(q)},p^{(r)})\boldsymbol{U}^+ \\ &+\mathcal{S}(p^{(m)},p^{(n)})\mathcal{S}^T(p^{(q)},p^{(r)})\boldsymbol{U}^-\Big]\end{aligned} \tag{15}$$

where $\boldsymbol{U}^+ = \boldsymbol{I}_2 \otimes (\boldsymbol{I}_M + \boldsymbol{J}_M)$ and $\boldsymbol{U}^- = \boldsymbol{I}_2 \otimes (\boldsymbol{I}_M - \boldsymbol{J}_M)$. The quantity $\eta^{(-,+)}_{mnqr}$ is equivalently defined by swapping $\boldsymbol{U}^+$ and $\boldsymbol{U}^-$. Furthermore, $p^{(0)}$ and $p^{(1)}$ refer resp. to $p[n]$ and $p'[n]$.

7. REFERENCES

[1] Behrouz Farhang-Boroujeny, "OFDM versus filter bank multicarrier," *IEEE Signal Processing Magazine*, vol. 28, no. 3, pp. 92–112, May 2011.

[2] M. Tanda et al., "Deliverable 2.1, Data-aided synchronization and initialization (single antenna)," Tech. Rep., ICT-211887 PHYDYAS, July 2008.

[3] Xavier Mestre, Marc Majoral, and Stephan Pfletschinger, "An asymptotic approach to parallel equalization of filter bank based multicarrier signals," *IEEE Transactions on Signal Processing*, vol. 61, no. 14, pp. 3592–3606, 2013.

[4] Tero Ihalainen, Tobias Hidalgo Stitz, Mika Rinne, and Markku Renfors, "Channel equalization in filter bank based multicarrier modulation for wireless communications," *EURASIP Journal on Applied Signal Processing*, vol. 2007, no. 1, pp. 140–140, 2007.

[5] D. Waldhauser, L. Baltar, and J. Nossek, "MMSE subcarrier equalization for filter bank based multicarrier systems," in *IEEE 9th Workshop on Signal Processing Advances in Wireless Communications, 2008. SPAWC 2008*. IEEE, 2008, pp. 525–529.

[6] L. Baltar, D. Waldhauser, J. Nossek, et al., "MMSE subchannel decision feedback equalization for filter bank based multicarrier systems," in *IEEE International Symposium on Circuits and Systems, 2009. ISCAS 2009*. IEEE, 2009, pp. 2802–2805.

[7] Aissa Ikhlef and Jérôme Louveaux, "An enhanced MMSE per subchannel equalizer for highly frequency selective channels for FBMC/OQAM systems," in *IEEE 10th Workshop on Signal Processing Advances in Wireless Communications, 2009. SPAWC'09*. IEEE, 2009, pp. 186–190.

[8] Tero Ihalainen, Aïssa Ikhlef, Jérôme Louveaux, and Markku Renfors, "Channel equalization for multi-antenna FBMC/OQAM receivers," *IEEE Transactions on Vehicular Technology*, vol. 60, no. 5, pp. 2070–2085, 2011.

[9] Marius Caus, Ana Pérez-Neira, et al., "Transmitter-receiver designs for highly frequency selective channels in MIMO FBMC systems," *IEEE Transactions on Signal Processing*, vol. 60, no. 12, pp. 6519–6532, 2012.

[10] Xavier Mestre and David Gregoratti, "A parallel processing approach to filterbank multicarrier MIMO transmission under strong frequency selectivity," in *2014 IEEE International Conference on Acoustics, Speech and Signal Processing (ICASSP)*. IEEE, 2014, pp. 8078–8082.

[11] Pierre Siohan, Cyrille Siclet, and Nicolas Lacaille, "Analysis and design of OFDM/OQAM systems based on filterbank theory," *IEEE Transactions on Signal Processing*, vol. 50, no. 5, pp. 1170–1183, 2002.

[12] Maurice G Bellanger, "Specification and design of a prototype filter for filter bank based multicarrier transmission," in *IEEE International Conference on Acoustics, Speech, and Signal Processing*. IEEE, 2001, vol. 4, pp. 2417–2420.